Photosynthesis and photoprotection in mangroves under field conditions

J. M. CHEESEMAN,[1,3] L. B. HERENDEEN,[1] A. T. CHEESEMAN[1] & B. F. CLOUGH[2]

[1]*Department of Plant Biology, University of Illinois, 505 S. Goodwin Ave., Urbana, IL 61801, USA, and* [2]*Australian Institute of Marine Science, Cape Ferguson, PMB3, Townsville, Queensland, 4810 Australia*

ABSTRACT

Net CO_2 exchange and *in vivo* chlorophyll fluorescence were studied in mangrove (*Rhizophora stylosa*) leaves at a field site in Western Australia, and leaf samples were collected for the analysis of enzymes and substrates potentially involved in anti-oxidant photoprotection. Photosynthesis saturated at 900 μmol quanta m^{-2} s^{-1} and at no more than 7·5 μmol CO_2 m^{-2} s^{-1}. However, fluorescence analysis indicated no chronic photoinhibition: F_v:F_m was 0·8 shortly after sunset, and quantum efficiencies of PSII were high up to 500 μmol quanta m^{-2} s^{-1}. Electron flow through PSII was more than 3 times higher than electron consumption through Calvin cycle activity, however, even with photorespiration and temperature-dependent Rubisco specificities taken into account.

Acknowledging the growing body of literature attributing a role to antioxidant systems in photoprotection, we also assayed the activities of superoxide dismutase (SOD) and several enzymes potentially involved in H_2O_2 metabolism. Their levels of maximal potential activity were compared with those in greenhouse-grown mangroves (*R. mangle*), and growth chamber-grown peas. Monodehydroascorbate reductase activities were similar in all species, and glutathione reductase was lower, and ascorbate peroxidase ≈40% higher, in the mangroves. SOD activities in field-grown mangroves were more than 40 times those in peas.

Our results support the hypothesis that O_2 may be a significant sink for photochemically derived electrons under field conditions, and suggest an important role for O_2^- scavenging in photoprotection. However, when relative patterns are compared between species, imbalances between SOD and the other enzymes in the mangroves suggest that more components of the system (e.g. phenolics or peroxidases) are yet to be identified.

Key-words: *Rhizophora*; Rhizophoraceae; ascorbate peroxidase; Mehler reaction; oxidative stress; photoinhibition; superoxide dismutase.

INTRODUCTION

Though the total global area occupied by mangroves is rel-

atively small, reflecting their restriction to tropical coasts, their ecological and sociological importance is unquestionable. As 'energy traps' and 'nurse ecosystems', mangroves are the primary producers and reproductive zones which shelter and feed juvenile populations of many off-shore species, including those which determine coral reef dynamics and many which are heavily exploited commercially (Redfield 1982; Tomlinson 1986). Throughout much of the tropics, mangroves also have significant local economic importance as sources of timber, pulp and firewood, as natural or manipulated fisheries, and as potential agricultural land (Tomlinson 1986).

Mangroves are physiologically interesting as potential models for stress tolerance and as sources of alternative ideas about physiological strategies relevant at the ecosystem level. They not only survive, but they dominate a harsh ecosystem. Even in areas with pronounced seasonality, most species maintain active leaves under conditions which might be expected to reduce severely photosynthetic capacity through photoinhibition. Indeed, this aspect of their photosynthetic metabolism might be critical to their sustained productivity throughout the year, but even the occurrence of photoinhibition in mangroves is a matter of question. Björkman and co-workers, for example, reported a large decrease in F_v:F_m when leaves of a number of mangroves, including *Rhizophora stylosa*, were directly illuminated in the field (Björkman, Demmig & Andrews 1988) while Cheeseman *et al.* reported no evidence of photoinhibition in exposed leaves of *Bruguiera parviflora* under natural illumination (Cheeseman *et al.* 1991) or in *Rhizophora mangle* under greenhouse, water-stressed conditions (Cheeseman 1994).

In this report, we extend our previous study of mangrove photosynthesis under field conditions in tropical Australia, with particular attention to the mechanisms of protection of the photosynthetic machinery against the potentially damaging effects of excess photons, excess electrons and active oxygen species.

MATERIALS AND METHODS

The field site

These studies were conducted in October/November 1994, at a field site near Karratha on the north-west coast of Western Australia. The site was located on the straight

Correspondence: John M. Cheeseman, Department of Plant Biology, University of Illinois, 505 S. Goodwin Ave., Urbana, IL 61801, USA.

between West Intercourse Island and the mainland and was bordered on the east by a levy. The adjacent land area is a semi-desert. Annual rainfall averages less than 30 cm, generally falling as isolated showers between late January and early March; the last measurable rain fell in February 1994. The site was tidally flooded twice daily to a depth of about 1 m.

Unless otherwise noted, all sampling was performed at the top of a 6 m canopy dominated by *Rhizophora stylosa* and *Avicennia marina*. Access to the canopy was by way of a scaffold tower erected at the beginning of the study. The tower was connected to the levy via a walkway. The site was chosen such that minimal damage to the trees would result from the erection of these structures. Four individual *R. stylosa* trees were accessible from the tower; there was no discrimination between them in analysing the results.

Other plant material

For purposes of putting the enzyme activities we will report for *R. stylosa* field samples into some context, a number of comparative assays were performed using greenhouse-grown *Rhizophora mangle* (a western hemisphere species similar to *R. stylosa*), or growth chamber-grown peas. The greenhouse trees were 5 to 7 years old, and were maintained in a room set to remain between 30 and 35 °C. The glass was uncoated, and the plants received full sunlight for about 3 h at midday. The growth chamber plants experienced a 14 h photoperiod with temperatures of 25 °C (day) and 20 °C (night). There was no humidity control. Irradiance at the top of the plants was ≈400 μmol quanta m^{-2} s^{-1}. Recently fully expanded leaves were sampled from all plants.

Gas exchange and fluorometry

Net CO_2 exchange was measured using a LiCor LI-6200 portable photosynthesis system with a locally designed, clamp-on, open-topped leaf chamber enclosing 6·25 cm^2 of leaf. Irradiance was measured using a Hamamatsu S4160–01 silicon photodiode, calibrated against the LiCor sensor and placed within 1 cm of the edge of the enclosed leaf area. A clamp mounted on the chamber accommodated the fibreoptic probe of the Walz PAM-2000 fluorometer.

The volume of the actual leaf chamber, a mixing chamber and gas lines was limited to 260 cm^3 in order to increase sensitivity at low rates of CO_2 exchange while reducing measurement noise and CO_2 depletion at higher rates. Preliminary statistical analyses of the LiCor signal fluctuations in the absence of a leaf in the chamber indicated that measurements of assimilation should be accurate to within 10% at rates of 2 μmol CO_2 m^{-2} s^{-1}, even in short sampling periods (J. M. Cheeseman, unpublished results). The chamber was designed for one-handed operation with a clamp that could be closed gently, preventing pressure transients or mechanical disturbance of the leaf. In greenhouse trials under benign conditions (25 to 28 °C), the chamber could be applied and detached repeatedly without changing net CO_2 exchange. Under high-temperature conditions, however, mangrove leaves become highly sensitive to disturbance such that, even with gentle manipulation, net CO_2 exchange may decline rapidly, with or without stomatal closure, during photosynthesis measurements. To minimize the impact of this effect on the results, the duration of each gas exchange measurement was 20 s and each sample consisted of two determinations; the timing was a compromise between the need for longer times to increase accuracy and a tendency for leaf temperature to increase and stomata to close during the measurements. If there were substantial changes in leaf temperature, stomatal conductance or net assimilation between the two measurements, the data were not used.

Immediately following the gas exchange measurements, fluorescence parameters were measured using the PAM-2000 with operating system version 2·00. After the saturating flash and determination of F_m' and F_t, a black cloth was placed over the leaf so that a far-red pulse would be capable of fully oxidizing PSI; that pulse followed the saturating flash by 3 s, and F_o' was measured. The quantum yield of PSII was calculated as $(F_m' - F_t)/F_m'$, and the operating efficiency of PSII, or the quantum yield of PSII with all Q_A oxidized ($F_v':F_m'$), was calculated as $(F_m' - F_o')/F_m'$. The apparent rate of electron transport was calculated as

$$ETR = 0·5 \times 0·75 \times I \times Y, \tag{1}$$

where I is the incident irradiance and Y is the quantum yield of PSII (Genty, Briantais & Baker 1989). Equation 1 assumes an equal distribution of photons between the two photosystems and an absorptance of 0·75 (Cheeseman *et al.* 1991). When fluorescence and gas exchange were combined, the irradiance in these calculations was that reported by the Li-6200. Otherwise, irradiance was measured using the Walz Leaf-Clip Holder. As indicated by the high correlation between ETR and irradiance below 500 μmol m^{-2} s^{-1} in Fig. 4c, which includes data obtained using both protocols, the two measuring systems gave consistent results.

For $F_v:F_m$ measurements, data were collected after sunset and throughout the night on naturally dark-adapted leaves. No daytime dark adaptation studies were performed.

Biochemical sampling and measurements

For chlorophyll analyses, four leaf discs were harvested using a #2 cork borer; the total sampled area was 0·96 cm^2. Discs were placed immediately in microcentrifuge tubes and frozen on dry ice for transfer to a laboratory at Karratha College. Discs were extracted for 24 h with dimethyl sulphoxide (DMSO) in the dark at 65 °C. Absorbances were read at 710, 665 and 648 nm and chlorophyll concentrations calculated using the equations of Barnes *et al.* (1992). Though all the data will be reported on a leaf area basis, approximate conversions to a chlorophyll basis can be performed based on a mean total chlorophyll concentration of 0·37 ± 0·01 mmol m^{-2}; the a/b ratio was 3·1 ± 0·1.

From the same leaves, nine #6 cork borer discs with a total area of 10.0 cm^2 and weighing 0.75 g were harvested rapidly into pre-folded aluminium foil packets, and immediately frozen on dry ice. They were stored on dry ice or in a -80 °C freezer until analysis. Separate leaves were used for analyses of potential non-enzymatic scavengers (ascorbate, dehydroascorbate and glutathione) and enzymes (ascorbate peroxidase, glutathione reductase, monodehydroascorbate reductase and superoxide dismutase).

For assays of greenhouse-grown *R. mangle* and growth chamber-grown peas and sunflowers, discs were harvested directly into liquid N_2 for extraction.

Ascorbate and glutathione

Samples were transferred to a mortar containing liquid N_2 and a small amount of fine sand, and were ground to a fine powder, then extracted by continued grinding in 8 cm^3 of 10% trichloroacetic acid. Subsamples were centrifuged for 7.5 min at 13 000 r.p.m. to remove debris, and partially neutralized with NaOH. Ascorbate (Asc) was analysed using the procedure of Law, Charles & Halliwell (1983). In a second subsample, dehydroascorbate (DHA) was chemically reduced to Asc with dithiothreitol (DTT) and analysed for total Asc; DHA was determined by difference.

For determination of total glutathione (GSH), 400 mm^3 of extract were incubated with 50 mg polyvinlypolypyrrilidone (PVPP) on ice for an additional 7.5 min, and recentrifuged. GSH was estimated in the supernatant using the 5,5'-dithiobis-(2-nitrobenzoic acid) (DTNB) reduction procedure of Tietze (1969).

Enzyme extraction

Several of the enzymes representing three pathways potentially involved in the detoxification of active oxygen (Fig. 5) were assayed using frozen tissue samples approximately 7 months after their collection. The delay was necessitated by the need to develop a medium capable of extracting enzymes from *R. stylosa* in active form. Initial assays using a medium suitable for tobacco, conifers and greenhouse-grown *R. mangle* were unsuccessful. The suitability of the medium we eventually used was established based on a 'spinach killing test'. In this test, spinach was extracted for analysis of ribulose-1,5-bisphosphate carboxylase oxygenase (Rubisco) and assayed (modified procedure from Sharkey, Savitch & Butz 1991) with and without a small amount of added mangrove extract. Initially, *R. stylosa* extract instantly and completely killed the assay. In the final medium, spinach Rubisco activity was unaffected by mangrove additions.

The basic grinding buffer contained HEPES (100 mol m^{-3}, pH 7.6), MgCl$_2$ (20 mol m^{-3}), KHCO$_3$ (0.15 mol m^{-3}), KCl (50 mol m^{-3}) and ascorbate (1 mol m^{-3}); this was also used as the desalting buffer and the assay buffer for glutathione reductase. For protection against phenolics and other oxidants, β-mercaptoethanol (0.11% v/v), PVP-360 (2% w/v) and Triton X-100 (0.1% v/v) were added. Finally, the protease inhibitors antipain, chymostatin, leupeptin, pepstatin and PMSF (phenyl-methanesulphonyl fluoride) were included. Stock solutions of the inhibitors were prepared as follows: PMSF was 7 mg cm^{-3} in isopropanol; the others were 0.25 mg cm^{-3} in DMSO (antipain and chymostatin), water (leupeptin) or ethanol (pepstatin). Each stock was diluted 20-fold in the grinding buffer. While it is possible that fewer antiproteases would have sufficed, the initial medium contained leupeptin which was insufficient and the number of field samples available precluded more extensive refining of the medium. Samples were ground in liquid N_2 as above prior to addition of the complete buffer mixture. For both *Rhizophora* species, 4 cm^3 of buffer was used per 10 cm^2 leaf area. For pea and sunflower, 2 cm^3 were used with 4.45 cm^2 leaf material.

Following grinding, extracts were desalted with Sephadex G-25 spin columns made in 5 cm^3 syringes, equilibrated with the basic grinding buffer without additions (Rubisco assays were performed on non-desalted samples). If samples were frozen prior to assay, 15% glycerol was added. Frozen extracts were used only for the assay of glutathione reductase and monodehydroascorbate reductase.

Enzyme assays

All assays were performed at 25 °C, and for comparability to gas exchange and electron transport measurements, all results will be expressed as activities in μmol m^{-2} (leaf area) s^{-1}.

Ascorbate peroxidase (APx) was assayed in frozen desalted extracts using the procedure of Nakano & Asada (1981) by following the decrease in absorbance at 290 nm in a medium containing 50 mol m^{-3} K-phosphate (pH 7.0), 0.1 mol m^{-3} H$_2$O$_2$ and 0.5 mol m^{-3} Asc. Rates were calculated based on an extinction coefficient for Asc of 2.8 (mol m^{-3})$^{-1}$ cm^{-1}. Glutathione reductase (GSR) was assayed in desalted extracts, following the oxidation of NADPH at 340 nm in the basic grinding buffer supplemented with 1 mol m^{-3} oxidized glutathione and 0.2 mol m^{-3} NADPH (Foster & Hess 1980). Rates were calculated based on an extinction coefficient of 4.5 (mol m^{-3})$^{-1}$ cm^{-1} determined for this medium. Monodehydroascorbate reductase (MDHAR) was assayed in frozen desalted extracts by following the oxidation of NADH at 340 nm in a medium containing HEPES (50 mol m^{-3}, pH 7.6), 0.1 mol m^{-3} NADH, 2.5 mol m^{-3} Asc and 0.14 U ascorbate oxidase (Miyake & Asada 1992). The steady-state concentration of monodehydroascorbate (MDHA) in this medium is 2.1 mol m^{-3} (Miyake & Asada 1992), and rates were calculated based on an extinction coefficient of 6.2 (mol m^{-3})$^{-1}$ cm^{-1}.

Superoxide dismutase (SOD) was assayed polarographically in desalted extracts using the procedure of Marshall & Worsfold (1978) modified with the inclusion of amino-triazole (0.42 mg cm^{-3}) to inhibit catalase (Hodgson & Raison 1991). Activities were calculated as the rates of O$_2$ consumption associated with conversion of O$_2$ to O$_2^-$ to

H_2O_2 in the presence of nitroblue tetrazolium (NBT); with this procedure, the units are comparable to those used in the other assays. In the absence of SOD activity, NBT scavenges O_2^- and regenerates O_2 (zero net consumption) with the production of formazans; at high irradiances or over long periods of illumination, the NBT may be totally consumed giving the appearance of SOD activity when O_2 is no longer regenerated. Thus, irradiance at the reaction vessel was limited to 600 μmol m^{-2} s^{-1} which was sufficient to generate enough O_2^- to saturate the SOD; it was monitored behind the reaction vessel where a continuous decrease in intensity throughout the measurement confirmed that NBT was still present. As *R. stylosa* SOD activities were very high, care was taken that samples were sufficiently dilute that activities in the reaction vessel were non-saturating. Cu/Zn SOD activity was estimated by inhibiting it with 5 mol m^{-3} KCN in a parallel assay and subtracting the remaining activity from the total.

Miscellaneous

All reagents and enzymes were obtained from Sigma Chemical Co., St. Louis, MO. Statistical analyses were performed using Statview 4·1 (Abacus Concepts, Inc. Berkeley CA) for Macintosh.

RESULTS

Gas exchange and fluorescence data and samples for biochemical analyses were collected at the top of the 6 m canopy over a 2 week period in October/November 1994, throughout the photoperiod. During the study period, days were sunny with maximal irradiances of $\approx$2000 μmol m^{-2} s^{-1}; maximum air temperatures ranged from 35 to 44 °C during the day, with cooling to $\approx$25 °C at night. Leaf water potentials (pressure bomb) varied from $-2\cdot5$ MPa predawn to -5 MPa, constant throughout the day.

Gas exchange

For gas exchange, the combined data set consisted of 279 samples. Irradiances ranged from 23 to 2000 μmol quanta m^{-2} s^{-1}, conductances from 0·006 to 0·21 mol H2O m^{-2} s^{-1}, and leaf temperatures from 25 to 48 °C.

Figure 1 shows the data set for net CO_2 assimilation as a function of irradiance. As expected for data collected on wild species under field conditions, there was considerable scatter at all irradiances; this was not a result of errors in the measurements themselves or limitations of the gas analyser (see 'Materials and methods'). Because of the data set size, however, there was also a clear upper surface. Using the technique previously described (Cheeseman *et al.* 1991), we placed a complex hyperbola at the upper surface of the set, and a least-squares, non-linear fit through the data cloud using the complex hyperbolic model:

$$A_{pred} = \frac{P_{max} + (\phi I) - [(P_{max} + \phi I)^2 - 4\theta(\phi I P_{max})]^{0.5}}{2\theta} - R_d,$$

$$(2)$$
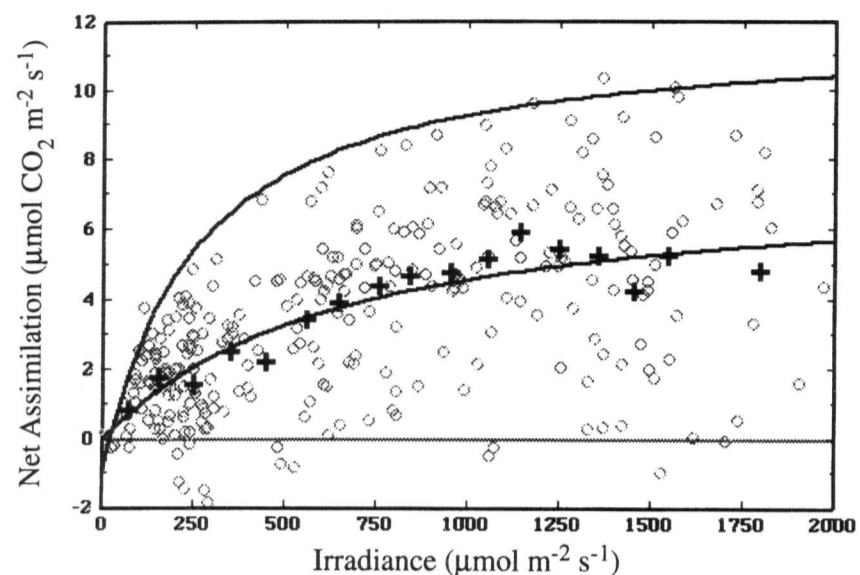
Figure 1. The irradiance dependence of net CO_2 assimilation in *Rhizophora stylosa* leaves under field conditions. o, complete data set ($n = 279$); +, data averaged over 100 μmol quanta m^{-2} s^{-1} intervals to 1500 μmol m^{-2} s^{-1} (all data combined for irradiances from 1500 to 2000 μmol m^{-2} s^{-1}). The upper curve was placed at the top of the data cloud using the procedure described by (Cheeseman *et al.* 1991): $\phi = 0\cdot058$, $\theta = 0\cdot100$, $P_{max} = 13\cdot0$, $R_d = 1\cdot2$. The lower curve was placed by non-linear regression: $\phi = 0\cdot011$, $\theta = 0\cdot126$, $P_{max} = 7\cdot5$, $R_d = 0\cdot05$. Both curves are of the form given by Eqn 2.

where A_{pred} is the predicted rate of assimilation (μmol CO_2 m^{-2} s^{-1}), P_{max} is the maximum rate, ϕ is the quantum efficiency at low light, θ is the convexity factor, R_d is respiration (the extrapolation of the light response to zero light) and I is incident irradiance (μmol quanta m^{-2} s^{-1}). Overall, the irradiance response in *R. stylosa* was similar to that reported previously in *Bruguiera* mangroves (Cheeseman *et al.* 1991), except that the convexity parameter was much lower in this case. Figure 1 also shows the mean values of assimilation averaged over intervals of 100 μmol quanta m^{-2} s^{-1} (the standard errors averaged 15% of these means). Using these values, the irradiance response was apparently linear to 1000 μmol m^{-2} s^{-1}, with a calculated efficiency of only 0·0049. Regardless of the method of analysis, however, there was clearly a saturation of net assimilation above about 900 μmol quanta m^{-2} s^{-1} (5·09 μmol CO_2 m^{-2} s^{-1}). This irradiance will be used to restrict data for 'high light' in later analyses.

Hidden in this figure is the fact that leaf temperatures tended to increase with irradiance. The mean T_{leaf} for irradiances below 100 μmol m^{-2} s^{-1}, for example, was 28 °C, increasing to 38 °C by 1300 μmol m^{-2} s^{-1}. Figure 2 summarizes the temperature response of light-saturated net assimilation ('high light'), dividing the data set into 2·5 °C intervals. Over the range of 30–48 °C, net assimilation decreased linearly with temperature.

Below 35 °C, the correlation between assimilation and conductance was insignificant. Between 35 and 42·5 °C, their relationship was linear and slopes were nearly identical regardless of the temperature interval. Above 42·5 °C, assimilation rates were too low to allow any meaningful correlations. Figure 3 shows the relationship between assimilation and conductance with the data restricted to
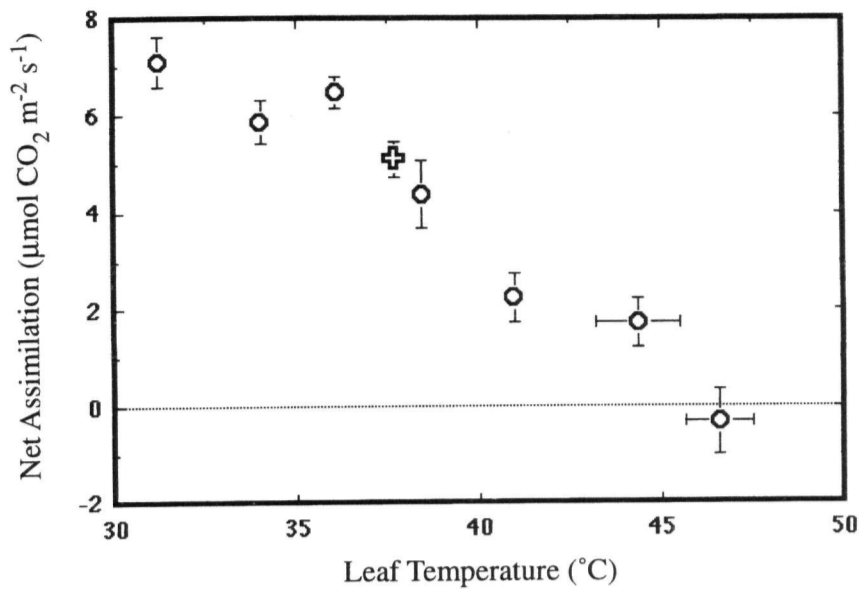
Figure 2. The temperature response of net assimilation in *R. stylosa* under field conditions, shown as the means of values averaged over 2·5 °C intervals. Over the range of 30–48 °C, net assimilation decreased linearly with temperature. o, means ± SE for each interval; +, mean for the intermediate (35 °C to 42·5 °C) range. Data were restricted to irradiances above 900 μmol m^{-2} s^{-1}.

high light between 35 and 42·5 °C. Hence, for subsequent analyses, we will define this as the 'intermediate temperature range'.

In order to consider further the effect of T_{leaf} on assimilation, we calculated total Calvin cycle electron consumption using the equations in the Appendix, using the effect of temperature on Rubisco specificity and solubilities of CO_2 and O_2 to determine photorespiratory contributions to the measurements. Over the intermediate temperature range at saturating light, the electrons consumed for a net fixation of one CO_2 increased linearly from 6·7 to 8·9 ($r^2 = 0.47$). The increase was not sufficient to eliminate correlations between photosynthesis and major environmental variables (Table 1), indicating that photorespiratory and photoassimilatory electron consumption did not vary in compensating ways such that total Calvin cycle electron usage at any irradiance was constant.

Besides irradiance, temperature and conductance, the final, basic, single-variable descriptor of photosynthetic characteristics is intercellular CO_2 (C_i). As in our *Bruguiera* studies (Cheeseman *et al.* 1991), the correlation between net CO_2 assimilation (or electron consumption) and C_i was highly significant and negative (Table 1). In stepwise regressions, at high light and intermediate temperatures and with the linear effects of conductance removed, the strong negative correlation with C_i could not be reduced by forced inclusion of other independent variables.

Fluorescence

The gas exchange data presented thus far were collected using a chamber on which the fibreoptic probe of the Walz PAM-2000 fluorometer could be mounted, and most of the measurements were followed by determination of PSII efficiency, oxidation of PSI (and Q_A) by far-red light, and subsequent determination of F_o'. Figure 4a shows the

relationship between incident irradiance and PSII efficiency for the set of measurements made at intermediate temperatures. Up to an irradiance of about 500 μmol m^{-2} s^{-1}, the data were tightly clumped around a mean of 0·69 (Table 2). Above 500 μmol m^{-2} s^{-1}, PSII efficiency dropped with increasing irradiance, to a mean of 0·30 above 900 μmol m^{-2} s^{-1}. The corresponding efficiencies of PSII with Q_A fully oxidized are shown in Fig. 4b. That the reductions in efficiency at high light were due to down-regulation of PSII rather than damage is indicated by the dark-adapted values of F_V:F_M (Table 2); within 30 min of sunset, F_V:F_M had recovered to 0·801, indicative of well-protected PSII activity. Combining the PSII efficiencies with absorbed irradiance and assuming equal partitioning of photons between the photosystems, the rate of electron transport through PSII was calculated using Eqn 1 (Fig. 4c). The low variability or PSII efficiency below 500 μmol m^{-2} s^{-1} is even more apparent in this presentation of the data.

Initial comparisons of ETR and either the net rate of CO_2 fixation or its associated rate of electron consumption indicated a very high degree of variability. This was probably due, in part, to limitations of the gas exchange system at low rates of net CO_2 assimilation (see 'Materials and
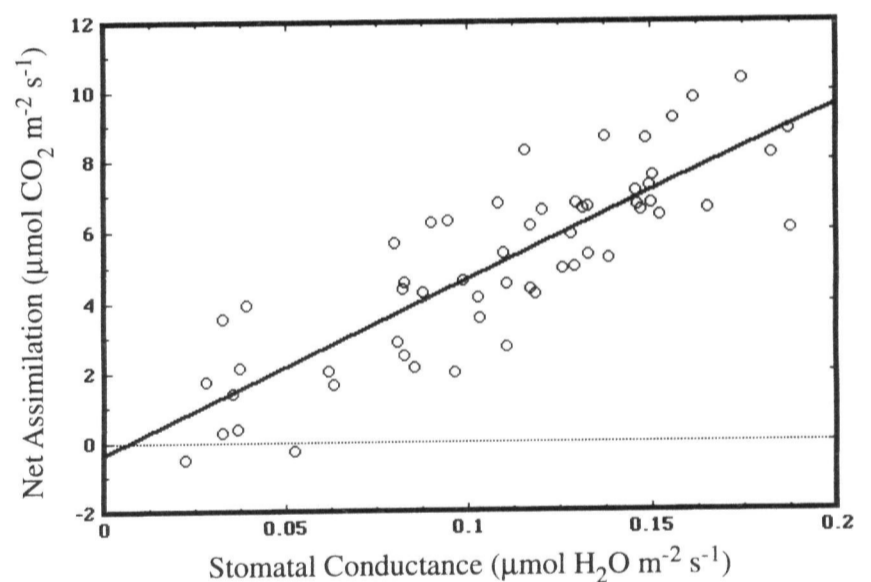
Figure 3. The dependence of net CO_2 assimilation on stomatal conductance in *R. stylosa* under field conditions. Data were restricted to intermediate temperatures (35 to 42·5 °C) and high light (above 900 μmol m^{-2} s^{-1}) for the analysis. The line was placed by linear regression: assimilation = –0·37 + 50·0 g_s ($r^2 = 0.71$).

Table 1. Correlation matrix for net CO_2 exchange, calculated Calvin cycle electron consumption and major variables expected to influence assimilation. Data for *Rhizophora stylosa* collected under field conditions in Western Australia were restricted to intermediate temperatures and irradiances above 900 μmol m^{-2} s^{-1} (n = 57)

	Net CO_2 exchange	Electron consumption
Irradiance	0·322	0·293
Leaf temperature	–0·654	–0·596
Stomatal conductance	0·844	0·757
Intracellular CO_2	–0·718	–0·803
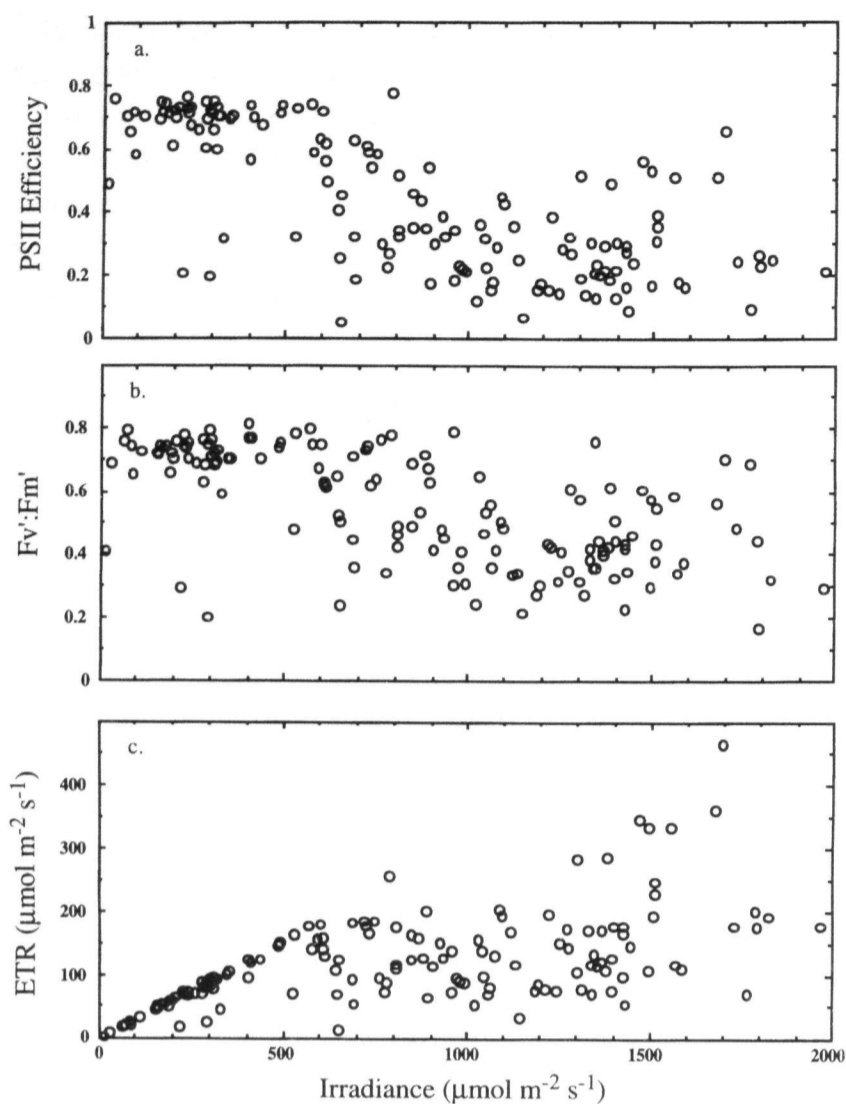
Figure 4. The dependence of three light-adapted fluorescence parameters on irradiance in *R. stylosa* under field conditions. For comparison to assimilation studies, data have been restricted to the intermediate temperature range (35 to 42·5 °C). In all cases, note the break in performance at ≈500 μmol quanta m^{-2} s^{-1}. (a) The photochemical efficiency of PSII; (b) PSII efficiency with Q_A fully oxidized by far-red light treatment; (c) electron transport rate calculated using Eqn 1 assuming a leaf absorptance of 0·75.

methods'). Therefore, still restricting the data to the intermediate T_{leaf} range, we limited net assimilation rates to 4 μmol CO$_2$ m^{-2} s^{-1} or greater, a range without statistical limitations on instrument accuracy. As shown in Table 3, with this restriction the mean calculated ETR (by fluorescence) was substantially higher than the calculated electron consumption; based on the averages of individual samples involving both measurements, electron flow provided more than 3 times the number of electrons accounted for by Calvin cycle activity. On the basis of CO$_2$ exchange alone, nearly 23 electrons were moved for each net CO$_2$ fixed. By comparison, in greenhouse *R. mangle* grown at high temperatures but supplied with ample water, the transport to consumption ratio was 2·2, with 14 electrons per CO$_2$ (Cheeseman 1994). Under drought stress, those ratios increased to 4·2 and 38, respectively.

At this point, based on recent literature, one likely acceptor of the excess electrons would be molecular O$_2$ (Miyake & Asada 1992; Hormann, Neubauer & Schreiber 1994; Lovelock & Winter 1996). Therefore, we supplemented the *in vivo* studies with assays of superoxide dismutase (SOD) and several enzymes potentially involved in H$_2$O$_2$ metabolism.

Anti-oxidant activities

Figure 5 illustrates the reactions responsible for production of superoxide and its subsequent detoxification in chloroplasts (recently reviewed by Allen 1995; Asada 1994b). O$_2^-$ may be scavenged directly and non-enzymatically, for example by reduced ascorbate or glutathione, or enzymatically by dismutation to H$_2$O$_2$ by SOD. Thereafter, three pathways have been studied for the reduction of the peroxide. Briefly, the first pathway entails the generation of MDHA by peroxidation of Asc (via APx), the disproportionation of the MDHA radical to DHA and Asc, and re-reduction of DHA through GSH and GSR. This pathway has generally been the most extensively studied and genetically manipulated (see Allen 1995 for a recent review), and we assayed GSR as an indicator of this mechanism. Alternatively, the MDHA radical may be directly reduced to Asc by MDHAR, which we assayed as an indicator of pathway 2 (Fig. 5). Finally, operating at or very close to thylakoid surfaces, the direct reduction of MDHA by Fd has received increasing attention in recent years and shows promise as a general mechanisms for O$_2^-$ detoxification. Lacking a method to isolate thylakoids and directly assay activity of this pathway in field-grown mangroves, we determined SOD and APx activities and compared them to the activities of the other indicator enzymes.

Table 2. Summary of fluorescence data for *Rhizophora stylosa* under field conditions in Western Australia. $F_v:F_m$ data were invariant between 30 min past sunset and 90 min after sunrise. Daytime data are grouped according to irradiance at the time of measurement

	Irradiance	Mean ± SE (n)
PSII efficiency	<500 μmol m^{-2} s^{-1}	0·691 ± 0·008 (235)
	>900 μmol m^{-2} s^{-1}	0·302 ± 0·013 (100)
$F_v':F_m'$	<500 μmol m^{-2} s^{-1}	0·733 ± 0·005 (232)
	>900 μmol m^{-2} s^{-1}	0·461 ± 0·013 (110)
$F_v:F_m$	dark-adapted	0·801 ± 0·004 (126)

Table 3. Summary of electron transport (based on fluorescence measurements) and electron consumption by Calvin cycle activities for *Rhizophora stylosa* leaves in the field in Western Australia. Data were restricted to intermediate leaf temperatures and to net assimilation rates greater than 4·0 μmol CO$_2$ m^{-2} s^{-1} and were included only if the measurements were performed together. Electron transport was calculated using Eqn 1; electron consumption by Eqn A6 (Appendix)

	Mean ± SE (n)
Electron transport rate	153 ± 12
Electron consumption rate (Calvin cycle)	48·6 ± 1·6
Electron transport/electron consumption (Calvin cycle)	3·3 ± 0·3
Electron consumption per net CO$_2$ fixed	6·97 ± 0·06
Electron transport per net CO$_2$ fixed	22·9 ± 1·8
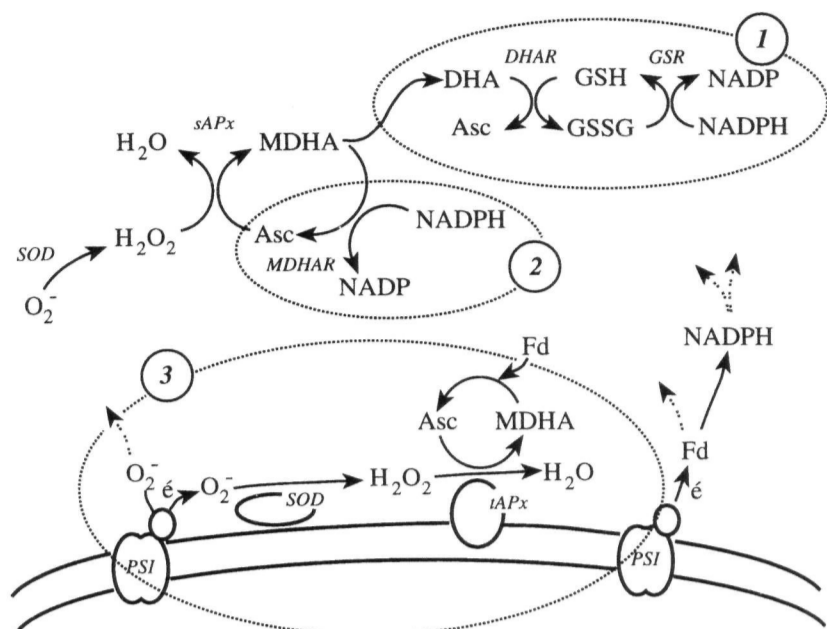
Figure 5. Potential pathways for superoxide detoxification in chloroplasts (redrawn from Allen 1995). O_2^- may be dismutated either by SOD in the stroma (alternatives 1 and 2) or by SOD closely associated with thylakoids at PSI (alternative 3). In turn, H_2O_2 may be scavenged by APx either at the thylakoid or in the stroma. Monodehydroascorbate (MDHA) may be disproportionated to DHA and Asc in the stroma (1), *or* it may be enzymatically reduced to Asc by MDHAR in the stroma (2), *or* it may be directly reduced by Fd at the thylakoid surface (3). DHA is re-reduced to Asc in the stroma via a series of redox couplings, with NADPH being the eventual electron donor.

Table 4 reports the levels of glutathione (GSH) and ascorbic acid (Asc) for *R. stylosa* leaves at the top of the canopy. GSH was present in a concentration of only about 0·2% of the Asc, suggesting that, if either were involved in non-enzymatic scavenging, the latter would be quantitatively far more significant. Regardless of the time of day or night, approximately half the Asc was in the oxidized, dehydroascorbate (DHA) form. In the mid-canopy, GSH concentrations were about 25% higher and Asc levels were about 15% lower; the oxidation states of Asc were similar.

Table 5 summarizes the activities of superoxide dismutase (SOD), ascorbate peroxidase (APx), glutathione reductase (GSR) and monodehydroascorbate reductase (MDHAR). Comparative data are included for *R. mangle* from the greenhouse collection at Illinois, and growth chamber-grown peas. In peas, the majority of the SOD activity was of the Cu/Zn form associated with chloroplasts; market spinach showed similar SOD activity (data not shown). Cu/Zn SOD activity was slightly greater than that of APx. Maximal GSR and MDHAR activities were 50 and 75% lower, respectively. In contrast, greenhouse-grown *R. mangle* had less than half the GSR activity and more than 6 times the total SOD activity of peas. Cu/Zn SOD was ≈2·5 times higher in the mangrove. APx was about 50% higher in *R. mangle*, while MDHAR levels were similar between the species. Field-grown *R. stylosa* had the lowest levels of GSR, one-sixth the activity found in pea, and MDHAR similar to values obtained for the other species. APx was equivalent to that in *R. mangle*. Clearly, the most striking difference was in SOD, with a total activity nearly 40 times higher than in peas; the activ-

ity of the Cu/Zn form was 25 times higher than in peas and 10 times higher than in the greenhouse-grown mangroves.

DISCUSSION

In this study, we have combined gas exchange, fluorescence and biochemical analyses to examine the photosynthetic performance of *Rhizophora stylosa* under extremely challenging field conditions. We have considered the relationships between absorbed irradiance, which appears as electron transport from PSII, the use of those electrons in Calvin cycle activity, and the protection of chloroplasts from what appears to be excess electrons. Overall, the fluorescence data for dark-adapted F_v:F_m confirm that mangrove chloroplasts are well protected against 'chronic photoinhibition' (*sensu* Osmond & Grace 1995) under field conditions, despite low rates of net CO_2 exchange. At this point, however, the results presented here cannot be unequivocally interpreted. The problems (discussed below) are exacerbated by the lack of comparable data for other species, either in controlled or field conditions, the lack of quantitative models of the reactions in Fig. 5 that would allow estimation of the degree of protection they afford, and the absence of coupled assay systems that would allow overall assessment of detoxification capacity. Even SOD activities are problematic as there are a number of non-equivalent assays used in the literature, and only one, that used here, gives results in units comparable to those of other photosynthetic processes.

Two areas in particular demand discussion: the question of excess electron transport, and, accepting that, the fate of the electrons. In studies of mature, unstressed crop species, the correspondence between electron flow calculated from fluorescence and CO_2 exchange has led to widespread acceptance of fluorescence as representing leaf-level photosynthetic activity (Baker 1996). However, the relationship is not absolute, particularly when there is environmental stress, and an alternative electron acceptor has been implicated (Baker, Oxborough & Andrews 1995). Excess electron transport capacity in chloroplasts has also long been recognized (e.g. Stitt 1986). Nevertheless, the transport/consumption imbalance in Table 3 is significantly larger than any previously reported (Loreto *et al.* 1994; Lovelock & Winter 1996; Osmond & Grace 1995), even after corrections for temperature effects on Rubisco specificity and gas solubilities. Our calculations clearly depend

Table 4. Concentrations of total glutathione, total ascorbate (ascorbate + dehydroascorbate) and the percentage of the total ascorbate present in the reduced form, for *Rhizophora stylosa* collected in the field in Western Australia. Data are expressed per volume of tissue water, and are means ± SE (*n*). Data can be converted to a leaf area basis by multiplying by $6·1 \, l \, m^{-2}$

	[GSH] (mmol m^{-3})	[Σ Ascorbate] (mol m^{-3})	[Asc]/[Σ Asc] (%)
R. stylosa	18·3 ± 0·7 (92)	8·4 ± 0·2 (92)	46 ± 1

Table 5. Activities of superoxide dismutase (SOD), ascorbate peroxidase (APx), glutathione reductase (GSR) and monodehydroascorbate reductase (MDHAR) from *Rhizophora stylosa*, *R. mangle* and peas. %Cu/Zn indicates the portion of the total SOD activity which was inhibited by 5 mol m^{-3} KCN, and hence was attributable to Cu/Zn SOD in chloroplasts. *R. stylosa* samples were collected in the field in Western Australia; *R. mangle* was grown in the Plant Biology greenhouses at the University of Illinois and the peas were grown in growth chambers (see 'Materials and methods'). Data are means ± SE (*n*)

Species	Total SOD	%Cu/Zn	APx	GSR	MDHAR
R. stylosa	639 ± 35 (46)	56 ± 3	16·4 ± 2·1 (44)	0·95 ± 0·13 (45)	2·94 ± 0·29 (46)
R. mangle	106 ± 15 (5)	34 ± 18	17·0 ± 1·4 (14)	2·1 ± 0·3 (14)	3·31 ± 0·19 (2)
P. sativum	16·7 ± 5·4 (4)	86 ± 9	11·6 ± 1·0 (13)	5·7 ± 2·5 (3)	3·02 ± 0·26 (5)

on the accuracy of both measurement techniques, and the large imbalance demands consideration of possible artifacts.

With respect to the gas exchange measurements, errors due to the instrumentation or field data collection *per se* were minimized through chamber and sampling protocol design (see 'Materials and methods'). Data for Table 3 were additionally restricted to minimize instrumentation errors, and temperature-compensated. Two additional factors for which we have made no corrections are cuticular conductance and mesophyll transfer conductance (see Cheeseman & Lexa 1996 for a recent review); both are functions of leaf anatomy. Both of the mangrove species used here have thick cuticles and multiple epidermes on both surfaces. As summarized by Nobel (1991, table 8·1), xerophyte cuticular conductances range from 0·4 to 4 mmol m^{-2} s^{-1}, at least an order of magnitude lower than the stomatal conductances in Fig. 3. Thus, cuticular conductance effects can be discounted. The mesophyll cell arrangements are relatively open and the leaves are homobaric (J. M. Cheeseman, unpublished results). Though we have no direct estimate of mesophyll conductance, they are unlikely to be less than those of other C$_3$ trees. But since any resistance to gas diffusion within the mesophyll would reduce the concentration of CO$_2$ at the site of fixation, any errors due to our neglecting this factor would be in the wrong direction, i.e. electron consumption would be overestimated.

With respect to the fluorescence studies, regardless of species, the signal will be dominated by chloroplasts nearer the illuminated surface. Though this could lead to artifacts when the ETR estimated from fluorescence is compared with gas exchange measurements, the following arguments indicate that the discrepancy between estimated ETR and CO$_2$ fixation cannot be explained in this way. At low incident irradiances, one would expect chloroplasts throughout the leaf to show little down-regulation, high photochemical efficiency of PSII, and low non-photochemical quenching. In that case, the total absorbed irradiance would be translated equally efficiently into electron flow, regardless of the mesophyll anatomy. The results in Fig. 4 for irradiances less than 500 μmol quanta m^{-2} s^{-1} would be expected. At higher irradiances, chloroplasts nearest the surface would be most strongly down-regulated. Though this would be a source of errors, the surface-based estimates should be the minimal rates likely. Thus, if

our transport/consumption estimate (Table 3) is incorrect, it is likely to be underestimated.

There are a number of possible fates for the excess electrons. Some of these, for example nitrite or sulphate reduction, are likely to be insignificant, especially in a nutrient-limited ecosystem. Reduction of oxaloacetate to malate may have greater quantitative potential and could be a source of electrons for other cellular- and tissue-level processes. In greenhouse studies of *R. mangle,* we have found leaf malate concentrations to rise more than 20-fold to 18 mol m^{-3} (tissue water basis) under drought stress, with afternoon levels slightly higher than morning levels (E. Carey & J. Cheeseman, unpublished results). Alternately, electrons could be cycled around PSII (Horton *et al.* 1989) or PSI. There is, so far, little agreement on the capacity of PSII cycling, especially at high irradiances. Hormann *et al.* (1994) have examined the possibility of PSI cycling and concluded that the overall capacity of the Mehler reaction and associated processes probably has, quantitatively, much greater potential.

At this point, none of these alternatives has been explored in any intact system, let alone under natural environmental conditions, and for this study we chose to concentrate on one that has, i.e. the delivery of electrons to molecular O$_2$ and the subsequent detoxification of O$_2^-$. In theory, superoxide can be scavenged in a number of ways, including by direct reaction with glutathione and ascorbate. Our results suggest that ascorbate scavenging may be possible in mangroves, based on its high concentration in the whole leaves, though the constant levels and constant ratio of Asc to DHA throughout the diurnal cycle make a firmer conclusion impossible.

Unquestionably, the bulk of recent attention to oxygen stress has been directed toward enzymatic detoxification of O$_2^-$, including molecular manipulation of enzymes in each of the pathways in Fig. 5 (see Asada 1994a,b; Allen 1995 for recent reviews; Bowler, van Montagu & Inzé 1992). To date, there has been mixed success in increasing stress tolerance through these constructions (Allen 1995), and only one study has included field trials of manipulated plants (McKersie *et al.* 1996). In that case, increasing total leaf SOD by only 2·5-fold led to improved short-term drought resistance and higher survivability and yield in alfalfa over 3 years of growth in the field. While direct comparison of SOD activities between studies is problematic because of differences in the assays, the SOD activities in peas and

mangroves (Table 5) are more than an order of magnitude greater than those available through genetic manipulations.

Of the post-SOD pathways, recent studies of direct photoreduction of MDHA in spinach thylakoids (Miyake & Asada 1992, 1994; Hormann *et al.* 1994) have led to increasing popularity of the thylakoid-localization hypothesis (pathway 3 in Fig. 5; Osmond & Grace 1995). Based only on the disparity between the maximal extractable activities of APx and those of GSR and MDHAR, representatives of the other two pathways, our data could be interpreted to support this hypothesis. In peas (Table 5) and in market spinach (data not shown), SOD would appear to be 'in balance' for this hypothesis. However, in both mangroves, this argument would imply a substantial imbalance between SOD and the rest of the enzymatic pathways. This transfers the problem of scavenging from O_2^- to H_2O_2, implying that none of the mechanisms is sufficient, and creating a need for alternative or additional peroxidase capacities. While no such models have been proposed using any species, peroxide-dependent oxidation of phenolics has been studied in spinach, both in chloroplasts and in the apoplast of leaves (Takahama 1984; Takahama & Oniki 1992), and *R. stylosa* leaves contain up to 20% by dry weight of such compounds, particularly under stressed conditions (Robertson 1988; Lovelock, Clough & Woodrow 1992).

In conclusion, the results of this study confirm the effective protection of mangrove photosynthetic systems from damage associated with excess irradiance under field conditions. The protection is effective even when excess electron transport is indicated. It is likely to be mediated, in large part, by processes beginning with the Mehler reaction, followed either by non-enzymatic scavenging of O_2^- by ascorbate, or by enzymatic detoxification through SOD. H_2O_2 is subsequently consumed either by a suite of enzymes within chloroplasts, or by peroxidase-mediated oxidation elsewhere in the leaf. Though a complete mechanistic model is still beyond the scope of our data, the details of an integrated and successful mechanism for photoprotection under stress clearly warrant further attention.

ACKNOWLEDGMENTS

REFERENCES

Allen R.D. (1995) Dissection of oxidative stress tolerance using transgenic plants. *Plant Physiology* **107**, 1049–1054.

Asada K. (1994a) Mechanism of radical scavenging in chloroplasts under light stress. In *Photoinhibition of Photosynthesis – from Molecular Mechanisms to the Field* (ed. N. R. Baker & J. R. Bowyer), pp. 129–142. Bios Scientific Publishers, Oxford.

Asada K. (1994b) Production and action of active oxygen species in photosynthetic tissues. In *Causes of Photooxidative Stress and Amelioration of Defense Systems in Plants* (ed. C. H. Foyer & P. M. Mullineaux), pp. 106–126. CRC Press, Boca Raton, FL.

Baker N.R. (1996) Environmental constraints on photosynthesis: an overview of some future prospects. In *Photosynthesis and the Environment* (ed. N. R. Baker), in press. Kluwer Academic Press, Dordrecht.

Baker N.R., Oxborough K. & Andrews J.R. (1995) Operation of an alternative electron acceptor to CO_2 in maize crops during periods of low temperatures. In *Photosynthesis: from Light to Biosphere* (ed. P. Mathis), pp. 771–776. Kluwer Academic Publishers, Dordrecht.

Barnes J.D., Balaguer L., Manrique E., Elvira S. & Davison A.W. (1992) A reappraisal of the use of DMSO for the extraction and determination of chlorophylls *a* and *b* in lichens and higher plants. *Environmental and Experimental Botany* **32**, 85–100.

Björkman O., Demmig B. & Andrews T.J. (1988) Mangrove photosynthesis: response to high-irradiance stress. *Australian Journal of Plant Physiology* **15**, 43–61.

Bowler C., van Montagu M. & Inzé D. (1992) Superoxide dismutase and stress tolerance. *Annual Review of Plant Physiology and Plant Molecular Biology* **43**, 83–116.

Brooks A. & Farquhar G.D. (1985) Effect of temperature on the CO_2/O_2 specificity of ribulose-1, 5-bisphosphate carboxylase/oxygenase and the rate of respiration in the light. *Planta* **165**, 397–406.

Cheeseman J.M. (1994) Depressions of photosynthesis in mangrove canopies. In *Photoinhibition of Photosynthesis – From Molecular Mechanisms to the Field* (ed. N. R. Baker & J. R. Bowyer), pp. 379–391. Bios Scientific Publishers, Oxford.

Cheeseman J.M., Clough B.F., Carter D.R., Lovelock C.E., Eong O.J. & Sim R.G. (1991) The analysis of photosynthetic performance in leaves under field conditions – a case study using *Bruguiera* mangroves. *Photosynthesis Research* **29**, 11–22.

Cheeseman J.M., Herendeen L.B., Cheeseman A.T. & Clough B.F. (1995) Antioxidant photoprotection in *Rhizophora* mangroves. In *Photosynthesis: from Light to Biosphere* (ed. P. Mathis), pp. 271–274. Kluwer Academic Publishers, Dordrecht.

Cheeseman J.M. & Lexa M. (1996) Gas exchange: models and measurements. In *Photosynthesis and the Environment* (ed. N. R. Baker), pp.

Dawson R.M.C., Elliott D.C., Elliott W.H. & Jones K.M. (1986) *Data for Biochemical Research*. Clarendon Press, Oxford.

Farquhar G.D., von Caemmerer S. & Berry J.A. (1980) A biochemical model of photosynthetic CO_2 assimilation in leaves of C3 species. *Planta* **149**, 78–90.

Foster J.G. & Hess J.L. (1980) Responses of superoxide dismutase and glutathione reductase activities in cotton leaf tissue exposed to an atmosphere enriched in oxygen. *Plant Physiology* **66**, 482–487.

Genty B., Briantais, J.-M. & Baker N.R. (1989) The relationship between the quantum yield of photosynthetic electron transport and quenching of chlorophyll fluorescence. *Biochimica et Biophysica Acta* **990**, 87–92.

Hodgson R.A.J. & Raison J.K. (1991) Lipid peroxidation and superoxide dismutase activity in relation to photoinhibition induced by chilling in moderate light. *Planta* **185**, 215–219.

Hormann H., Neubauer C. & Schreiber U. (1994) An active Mehler-peroxidase reaction sequence can prevent cyclic PS I electron transport in the presence of dioxygen in intact spinach chloroplasts. *Photosynthesis Research* **41**, 429–437.

Horton P., Crofts J., Gordon S., Oxborough K., Rees D. & Scholes J.D. (1989) Regulation of photosystem II by metabolic and environmental factors. *Philosophical Transactions of the Royal Society (London) series B* **323**, 269–279.

Law M.Y., Charles S.A. & Halliwell B. (1983) Glutathione and ascorbic acid in spinach (*Spinacia oleracea*) chloroplasts. The effect of hydrogen peroxide and paraquat. *Biochemistry Journal* **210**, 899–903.

Loreto F., Di Marco G., Tricoli D. & Sharkey T.D. (1994) Measurement of mesophyll conductance, photosynthetic electron transport and alternative electron sinks of field grown wheat leaves. *Photosynthesis Research* **41**, 397–403.

Lovelock C.E., Clough B.F. & Woodrow I.E. (1992) Distribution and accumulation of ultraviolet-radiation-absorbing compounds in leaves of tropical mangroves. *Planta* **188**, 143–154.

Lovelock C.E. & Winter K. (1996) Oxygen-dependent electron transport and protection from photoinhibition in leaves of tropical tree species. *Planta* **198**, 580–587.

Marshall M.J. & Worsfold M. (1978) Superoxide dismutase: a direct, continuous linear assay using the oxygen electrode. *Analytical Biochemistry* **86**, 561–573.

McKersie B.D., Bowley S.R., Harjanto E. & Leprince O. (1996) Water-deficit tolerance and field performance of transgenic alfalfa overexpressing superoxide dismutase. *Plant Physiology* **111**, 1177–1181.

Miyake C. & Asada K. (1992) Thylakoid bound ascorbate peroxidase in spinach chloroplasts and photoreduction of its primary oxidation product, monodehydroascorbate radicals in thylakoids. *Plant and Cell Physiology* **33**, 541–553.

Miyake C. & Asada K. (1994) Ferredoxin-dependent photoreduction of the monodehydroascorbate radical in spinach thylakoids. *Plant and Cell Physiology* **35**, 539–549.

Nakano Y. & Asada K. (1981) Hydrogen peroxide is scavenged by ascorbate-specific peroxidase in spinach chloroplasts. *Plant and Cell Physiology* **22**, 867–880.

Nobel P. (1991) *Physicochemical and Environmental Plant Physiology*. Academic Press, San Diego.

Osmond C.B. & Grace S.C. (1995) Perspectives on photoinhibition and photorespiration in the field: quintessential inefficiencies of the light and dark reactions of photosynthesis? *Journal of Experimental Botany* **46**, 1351–1362.

Redfield J.A. (1982) Trophic relationships in mangrove communities. In *Mangrove Ecosystems in Australia: Structure, Function and Management* (ed. B. F. Clough), pp. 259–262. Australian National University Press, Canberra.

Robertson A.I. (1988) Decomposition of mangrove leaf litter in tropical Australia. *Journal of Experimental Marine Biology and Ecology* **116**, 235–247.

Sharkey T.D., Savitch L.V. & Butz N.D. (1991) Photometric method for routine determination of K_{cat} and carbamylation of rubisco. *Photosynthesis Research* **28**, 41–48.

Stitt M. (1986) Limitation of photosynthesis by carbon metabolism. I. Evidence for excess electron transport capacity in leaves carrying out photosynthesis in saturating light and CO_2. *Plant Physiology* **81**, 1115–1122.

Takahama U. (1984) Hydrogen peroxide-dependent oxidation of flavonols by intact spinach chloroplasts. *Plant Physiology* **74**, 852–855.

Takahama U. & Oniki T. (1992) Regulation of peroxidase-dependent oxidation of phenolics in the apoplast of spinach leaves by ascorbate. *Plant and Cell Physiology* **33**, 379–387.

Tietze F. (1969) Enzymic method for quantitative determination of nanogram amounts of total and oxidized glutathione: applications to mammalian blood and other tissues. *Analytical Biochemistry* **27**, 502–522.

Tomlinson P.B. (1986) *The Botany of Mangroves*. Cambridge University Press, Cambridge.

APPENDIX

In order to estimate the number of electrons consumed by Calvin cycle activity from the gas exchange measurements, it was necessary to estimate the relative amounts of CO_2 and O_2 fixation by Rubisco, corrected for temperature and dissolved gas concentrations at the sites of fixation. Using Brooks & Farquhar's fitting of Jordan & Ogren's data on Rubisco specificity (Brooks & Farquhar 1985),

$$\Gamma_* = 44 \cdot 3 + 1 \cdot 88(T - 25) + 0 \cdot 036(T-25)^2, \tag{A1}$$

where Γ_* is the CO_2 compensation point in the absence of daytime respiration other than photorespiration. From this and the local concentration of O_2, the specificity, S, of Rubisco can be calculated:

$$S \equiv 0 \cdot 5 \times [O_2]/\Gamma_*. \tag{A2}$$

Then, the ratio of carboxylation to oxygenation, defined as ρ, is

$$\rho \equiv S \times \frac{[CO_2]}{[O_2]}. \tag{A3}$$

Both concentrations are those of the dissolved gasses, and depend on leaf temperature. The solubilities were calculated using cubic polynomials fit to the solubilities corrected for the actual partial pressures using the tables in Dawson *et al.* (1986). For O_2 at 210 mbar,

$$[O_2]\ (\text{mmol m}^{-3}) = 456 \cdot 25 - 11 \cdot 616\ T_{leaf} + 0 \cdot 183\ (T_{leaf})^2 - 0 \cdot 0011\ (T_{leaf})^3 \tag{A4a}$$

and for CO_2 at 350 μbar,

$$[CO_2]\ (\text{mmol m}^{-3}) = 26 \cdot 32 - 0 \cdot 901\ T_{leaf} + 0 \cdot 016\ (T_{leaf})^2 - 0 \cdot 000106\ (T_{leaf})^3. \tag{A4b}$$

The $[CO_2]$ was further corrected based on the gas analysis estimate of intracellular CO_2 (C_i) in the absence of further data on mesophyll conductance.

Finally, the rate of carboxylation was calculated as

$$V_c = (A + R_d)/(1 - \frac{0 \cdot 5}{\rho}), \tag{A5}$$

where R_d is day respiration (Farquhar, von Caemmerer & Berry 1980), assumed here to be 0.9 μmol CO_2 m^{-2} s^{-1}, and the associated consumption of electrons (NADPH) was

$$\text{é\_consumption} = (4 + \frac{4}{S}) \times V_c. \tag{A6}$$